TECHNICAL NOTE: ANALYSIS OF CONCENTRATION-DISCHARGE HYSTERESIS LOOPS USING SELF-ORGANIZING MAPS

AUTHORS' RESPONSE TO REFEREE 1

Responses in red

Overall, this manuscript is well written and supported with literature. You demonstrate strong scientific rigor, present informative figures, and provide a supportive narrative.

First and foremost, we sincerely appreciate your positive assessment of our manuscript. Your comments were both encouraging and helpful. We have carefully addressed your suggestions in the revised version, which we believe has improved the overall clarity and quality of the work.

Line 26: You mention that event-scale concentration has been employed for decades, but the oldest citation is only 5 years old (*Malutta et al., 2020*). Can you add some older/original literature in this first sentence to support your claim? Perhaps *Williams (1989), Hamshaw et al. (2018), Bettel et al. (2025)* since you mention in Line 225 that hysteresis loops were first recognized in these articles.

The citations originally included in this line are review papers that provide comprehensive discussions on concentration–discharge relationships, including its historical development. However, we agree it is valuable to cite some of the original, foundational studies to better support our claim. Accordingly, we will update the manuscript to include the following references:

Heidel, S. G. (1956). The progressive lag of sediment concentration with flood waves. Eos, Transactions American Geophysical Union, 37(1), 56–66.

Williams, G. P. (1989). Sediment concentration versus water discharge during single hydrologic events in rivers. Journal of Hydrology, 111(1), 89–106. https://doi.org/10.1016/0022-1694(89)90254-0

Evans, C., & Davies, T. D. (1998). Causes of concentration/discharge hysteresis and its potential as a tool for analysis of episode hydrochemistry. Water Resources Research, 34(1), 129–137. https://doi.org/10.1029/97WR01881

Section 2.2 – 2.4: I think these sections would be easier visualized with a workflow diagram that links to Figure 3. You could include a visualization for the process of training the model and finding the BMU. In the same workflow diagram, you can include a visualization for the process of using the DTW. Then, those can have an arrow pointing to the "SOM training" in Figure 3. Additionally, if possible, including the topological preservation and quantization accuracy into the diagram would help create a complete "picture" of the process. Although these three sections are written well, it is hard to visualize the order of the process. Additionally, Figure 3 in its current state is too general to provide a specific picture of the training process.

We agree that adding workflow diagrams will significantly enhance the clarity and visual structure of Sections 2.2 to 2.4. Accordingly, we have created three new diagrams to illustrate:

- The intuition behind the Dynamic Time Warping (DTW) algorithm and its distinction from Euclidean distance (Fig. 1).

- The workflow for training an individual Self-Organizing Map (SOM) (Fig. 2).
- The process for tuning SOM hyperparameters for hysteresis analysis, highlighting the role of quantization and topographic errors (Fig. 3).

Because DTW and SOM training algorithms are well-established and thoroughly described in the literature, we have opted to include Figures 1 and 2 in the Supplementary Material. In contrast, Figure 3 represents a methodological contribution tailored specifically to our use of SOMs for hysteresis analysis and will therefore be included in the main manuscript.

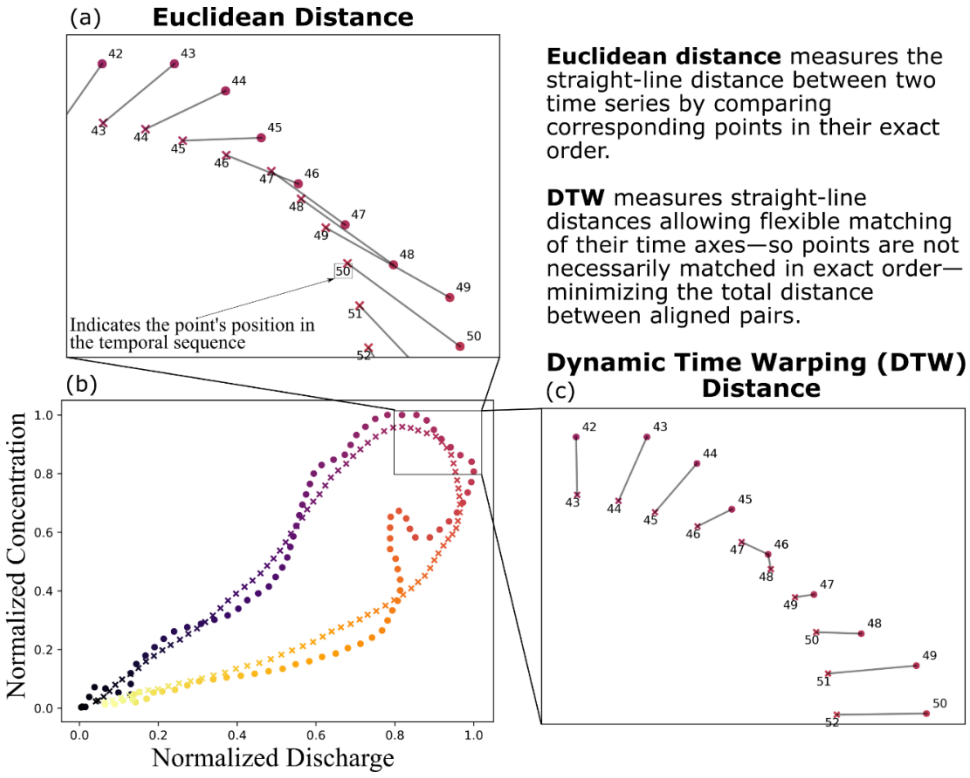

Figure 1. Comparison of Euclidean and Dynamic Time Warping (DTW) distances. The figure illustrates how DTW's flexible alignment yields smaller distance values than Euclidean distance when sequences (loops) follow similar paths but are temporally misaligned.

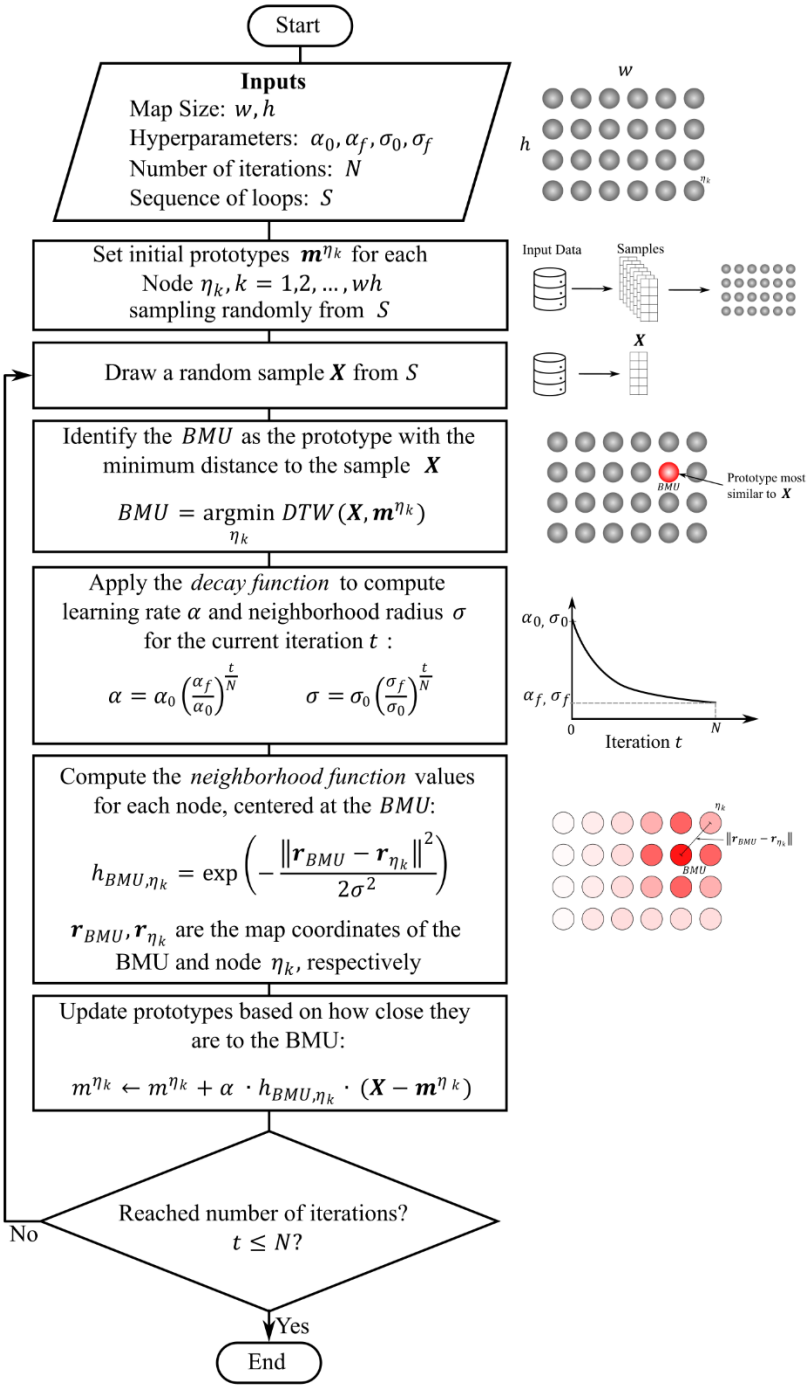

Figure 2. Workflow diagram illustrating the training process of a Self-Organizing Map. Parameters w and h represent the number of nodes along the horizontal and vertical dimensions. The learning rate α, starts at α_0 and gradually decreases to α_f following the decay function. Similarly, the neighborhood radius σ evolves from σ_0 to σ_f. All remaining symbols are defined within the diagram.

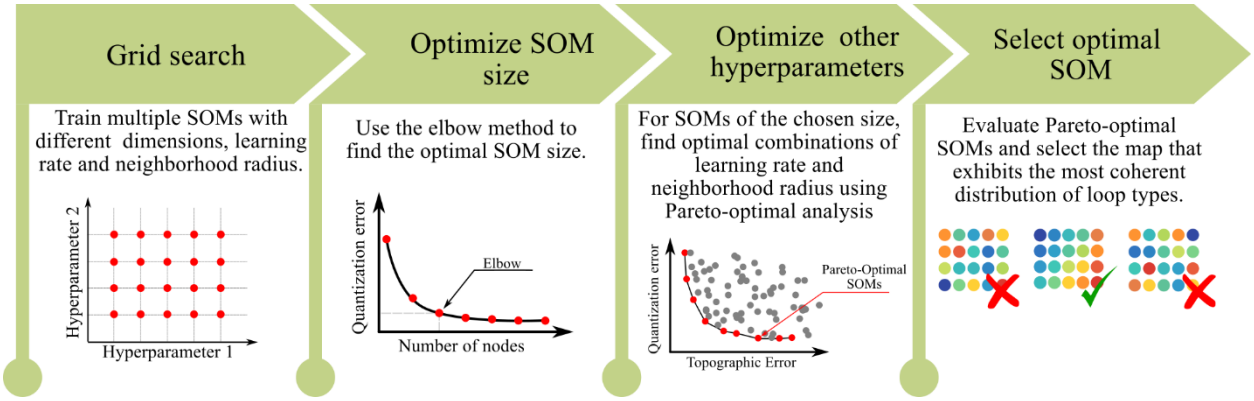

Figure 3. Workflow for tuning SOM hyperparameters. A grid search is used to train multiple SOMs with varying hyperparameter combinations. The resulting maps are then assessed to identify the optimal model. First, the best SOM dimensions are determined by locating the point beyond which increases in size yield no significant improvement in quantization error (elbow method). Next, Pareto-optimal SOMs with the selected dimensions are visually inspected to select the map with the most coherent distribution of loop types.

Line 228: I recommend simply adding a parenthesis such as (as seen on the left rows in Figure 4) after the sentence to immediately direct your viewers eyes to the single-line, clockwise, and counterclockwise.

We will modify the sentence as follows:
However, our analysis suggests that sediment hysteresis loop diversity can largely be explained by 17 loop types, encompassing different variations of single-line (first row in Fig. 4), clockwise (second row in Fig. 4), and counterclockwise (third row in Fig. 4) topologies.

Figure 4 caption: I would also recommend adding additional information on the single-line, Figure 8, clockwise, and counterclockwise topologies. You have a lot of detail in Figure 1-3, and I would suggest continuing that format.

We will modify the caption as follows:

Figure 4. Loop types considered in the training dataset. Except for Figure-L loops—introduced by Hamshaw et al. (2018)—all loop types were originally described by Williams (1989). We gathered 20 samples per loop type from 37 stream gages operated by the USGS across the United States. While past studies often lump together all subclasses within the broader categories of Single Line, Clockwise, and Counterclockwise loops, our dataset introduces a more granular classification that captures multiple shaper variations within each type, such as differences in concavity, which reflect the relative spread of the sedigraph with respect to the hydrograph, or Figure-L loops, which indicates strong decoupling between discharge and sediment concentration. Readers interested in the hydrological interpretation of these loop types are encouraged to consult the original studies.

Line 256: It seems like Line 256 should be appended to line 255.

We agree.

Line 259: Would the highly distorted maps be defined by topological error (e.g. referring to section 2.3) and not the "topographic" error that is listed? If so, topographic is used throughout the paper (Line 169 and Line 325, Line 327, etc.) and would need corrected.

The terms *topological preservation* and *topographic error* refer to related but distinct concepts. Topological preservation describes the abstract ability of a SOM to maintain relative distances between data points when projecting them from high-dimensional space to a two dimensional map. Topographic error, by contrast, is a specific metric used to quantify the degree of topological preservation achieved by a trained SOM. This distinction is explained in section 2.3:

> ***Topological preservation*** *ensures that the map maintains the neighborhood relationships of the input space. Hence, a good topological preservation indicates that similar prototypes are placed close to each other and dissimilar prototypes are placed farther apart.* ***Topological preservation can be quantified using the topographic error***.

Therefore, the correct term in this context is topographic error. However, we mistakenly used the term "topological error" on Line 157, and we have corrected this in the revised version.

Line 262: A citation should be provided for the Pareto-optimal analysis.

The following reference will be added where the Pareto-optimal analysis is thoroughly described

Koppa, A.; Gebremichael, M.; Yeh, W. W.-G. Multivariate Calibration of Large Scale Hydrologic Models: The Necessity and Value of a Pareto Optimal Approach. *Advances in Water Resources* **2019**, *130*, 129–146. https://doi.org/10.1016/j.advwatres.2019.06.005.

Figure 8 caption: Please provide an explanation of what is shown in (a), (b), (c), (d), specifically.

We will modify the caption as follows:

Figure 8. Mapping of all samples from the curated loop dataset (see Fig. 3) to their respective Best Matching Units (BMUs) on the Kohonen map. For visual clarity, loop types and their mappings are organized into four distinct panels: (a) single-line loops; (b) clockwise loops including Async, Sync, Concave, and Figure-L; (c) counterclockwise loops including Async, Sync, Concave, and Figure-L; and (d) Figure-8 and Line+ loops. Acronyms used in the figure include: SP – Sync-Peak, AP – Async-Peak, CU – Concave-Up, CD – Concave-Down, ccw – Counterclockwise, cw – Clockwise, fL – Figure-L, f8 – Figure 8.